

Supplemental information for:

A Photoactivated Ir(III) Complex Targets Cancer Stem Cells and Induces Secretion of Damage-associated Molecular Patterns in Melanoma Cells Characteristic of Immunogenic Cell Death

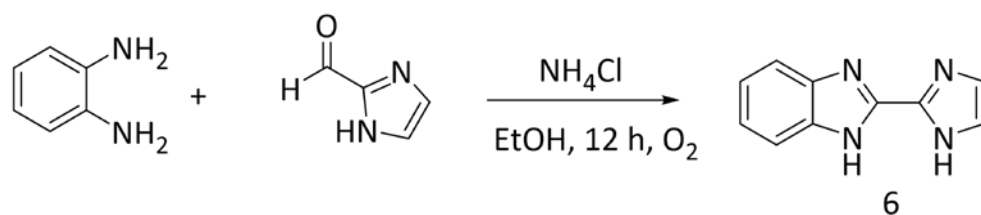
Gloria Vigueras,^{a,#} Lenka Markova,^{b,#} Vojtech Novohradsky,^b Alicia Marco,^a Natalia Cutillas,^a Hana Kostrhunova,^b Jana Kasparikova,^b José Ruiz,^{*,a} and Viktor Brabec^{*,b}

^a*Departamento de Química Inorgánica, Universidad de Murcia and Institute for Bio-Health Research of Murcia (IMIB-Arrixaca), E-30071 Murcia, Spain*

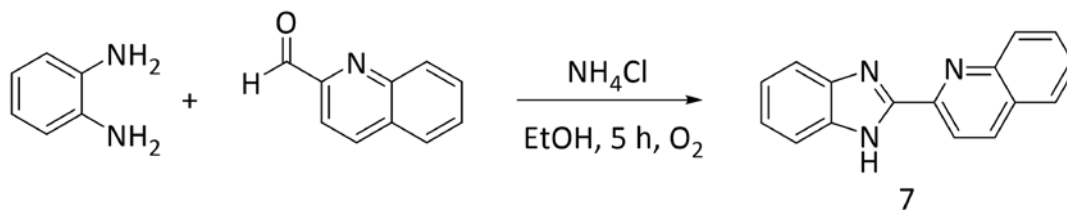
^b*Czech Academy of Sciences, Institute of Biophysics, Kralovopolska 135, CZ-61265 Brno, Czech Republic*

Table of Contents

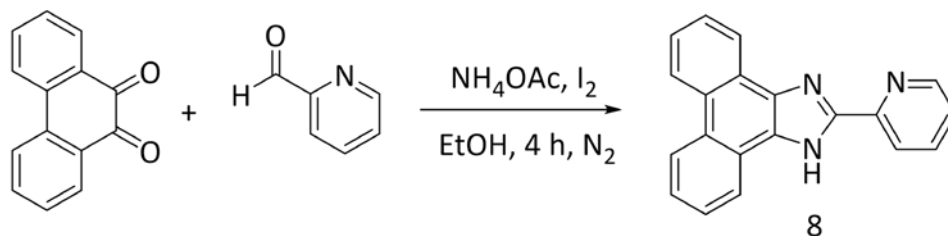
Synthesis of 6-8	S2
Route of synthesis of the new Ir(III) complexes	S2
¹ H and ¹³ C NMR spectra and HR ESI-MS of the compounds	S3-S8
RP-HPLC purity and stability analyses	S8
Photophysical characterization of the compounds	S9-S11
Photo-oxidation of NADH	S11-S12
Determining the lipophilicity by HPLC. Log <i>P</i> calculation	S13-S14
Antiproliferative and Phototoxicity Testing	S14
Ecto-Calreticulin exposure for A375 cells	S15
In vitro Phagocytosis Assay	S16
Penetration into 3D Spheroids.	S16-S17
Molecular Formula Strings	S18



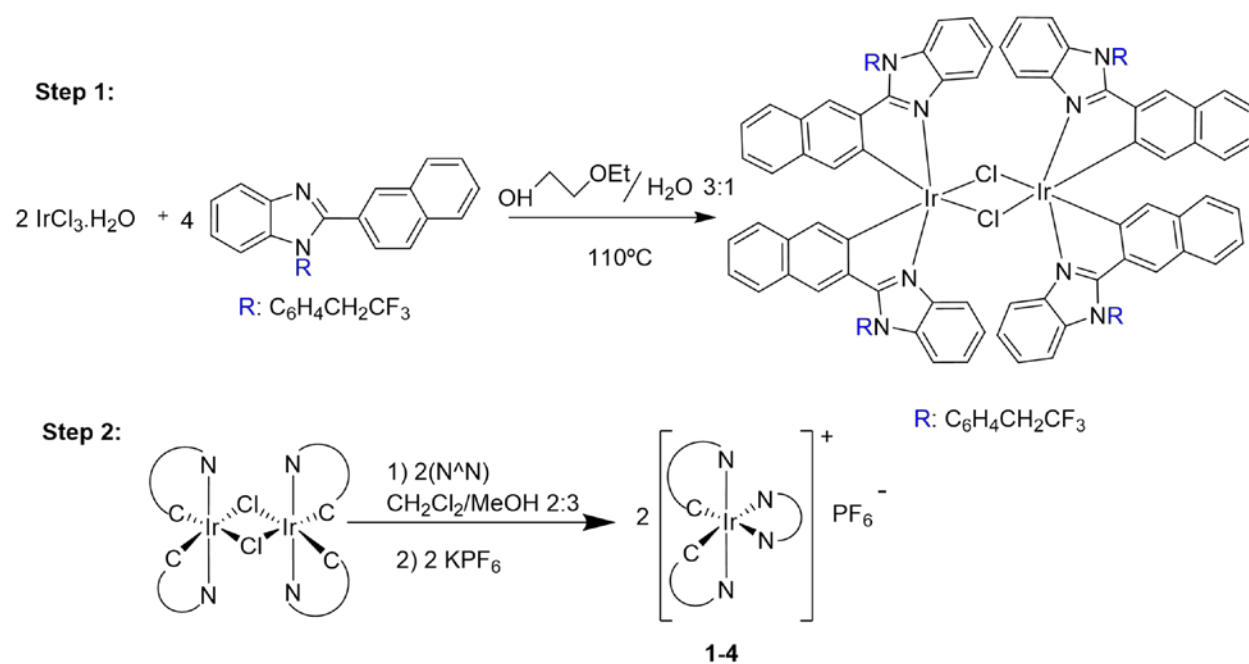
Scheme S1. Synthesis of **6**.



Scheme S2. Synthesis of **7**.



Scheme S3. Synthesis of **8**.



Scheme S4. Route of synthesis of the new Ir(III) complexes.

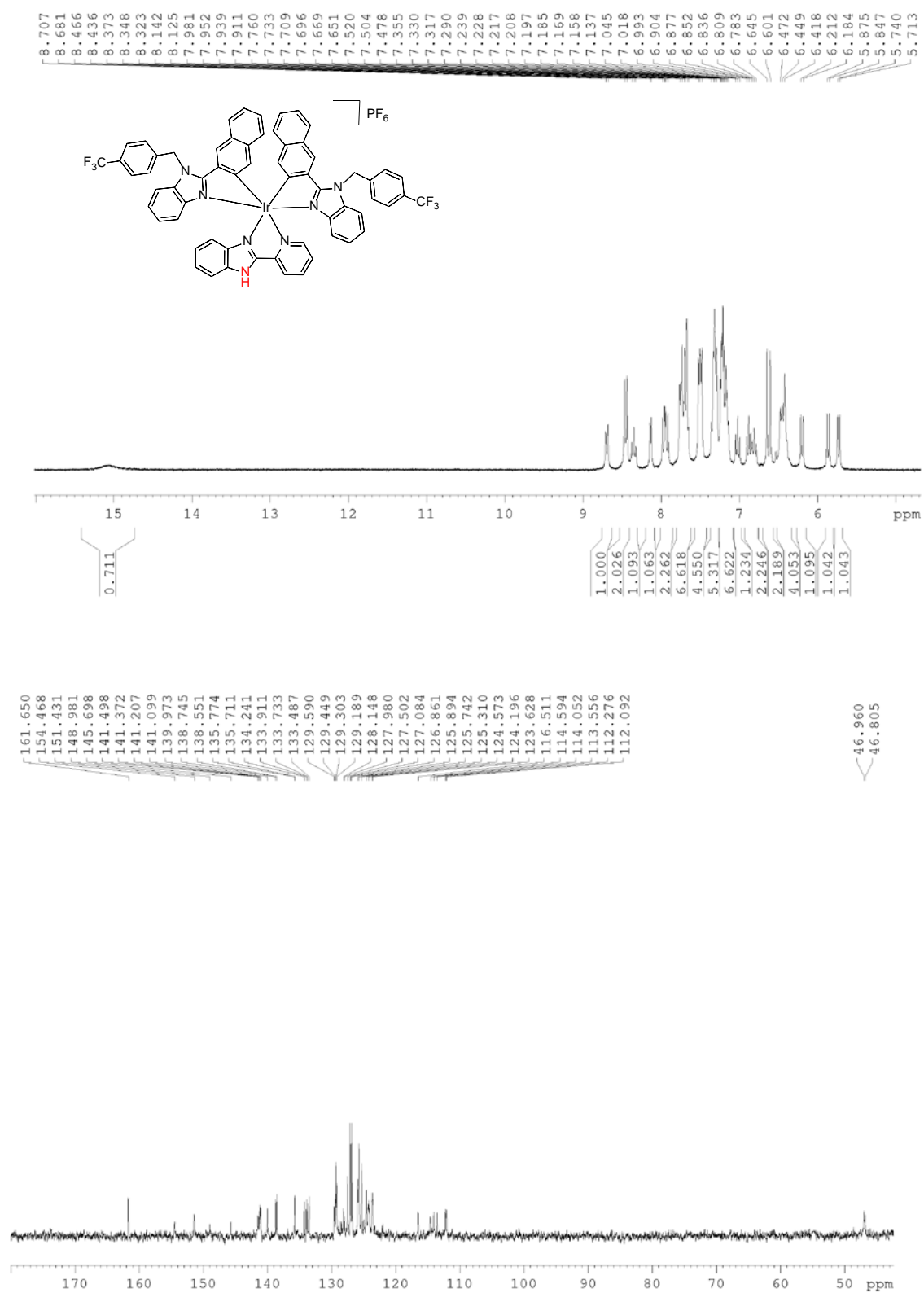


Figure S1. ¹H and ¹³C NMR in [D₆]DMSO for **1**.

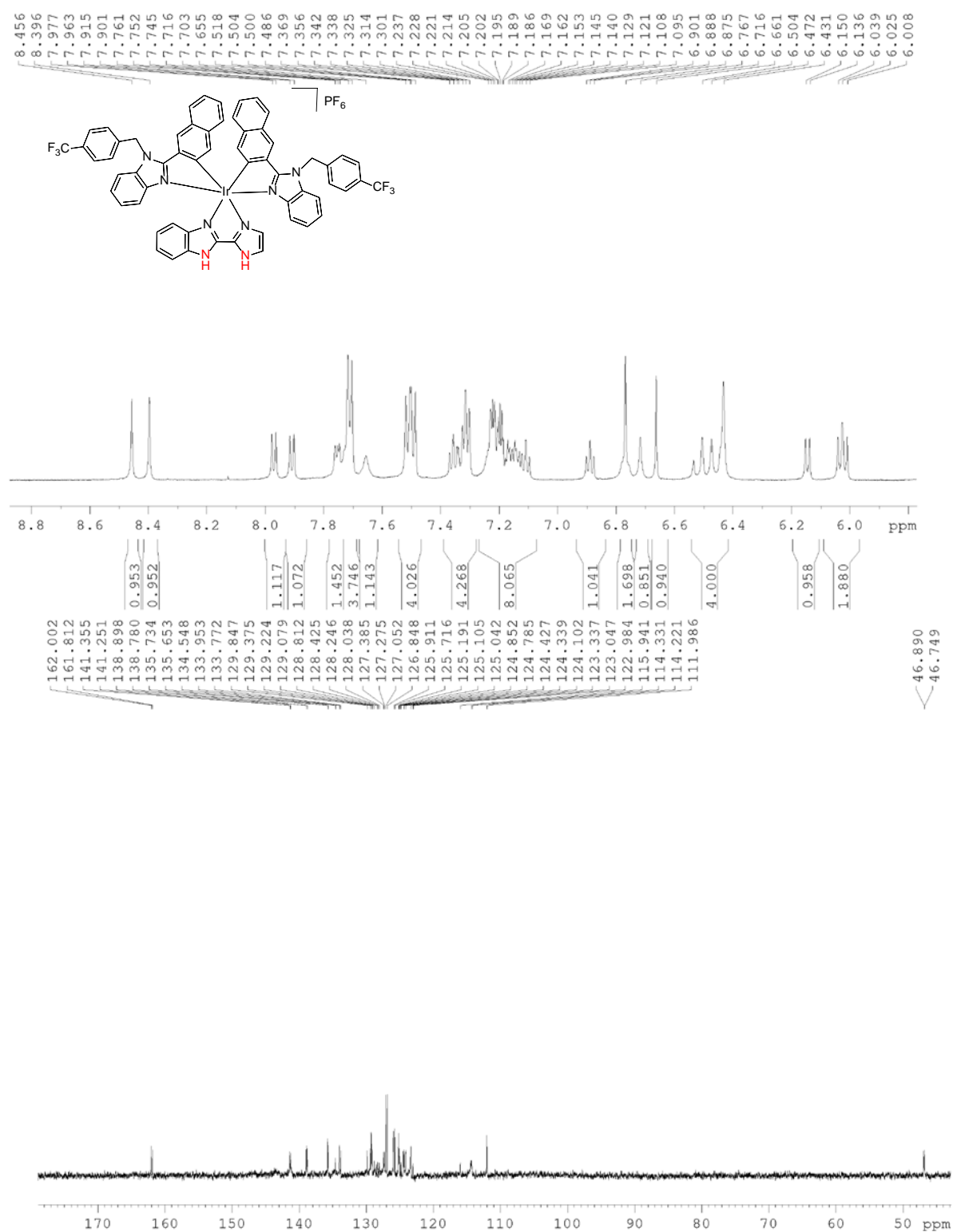


Figure S2. ¹H and ¹³C NMR in [D₆]DMSO for **2**.

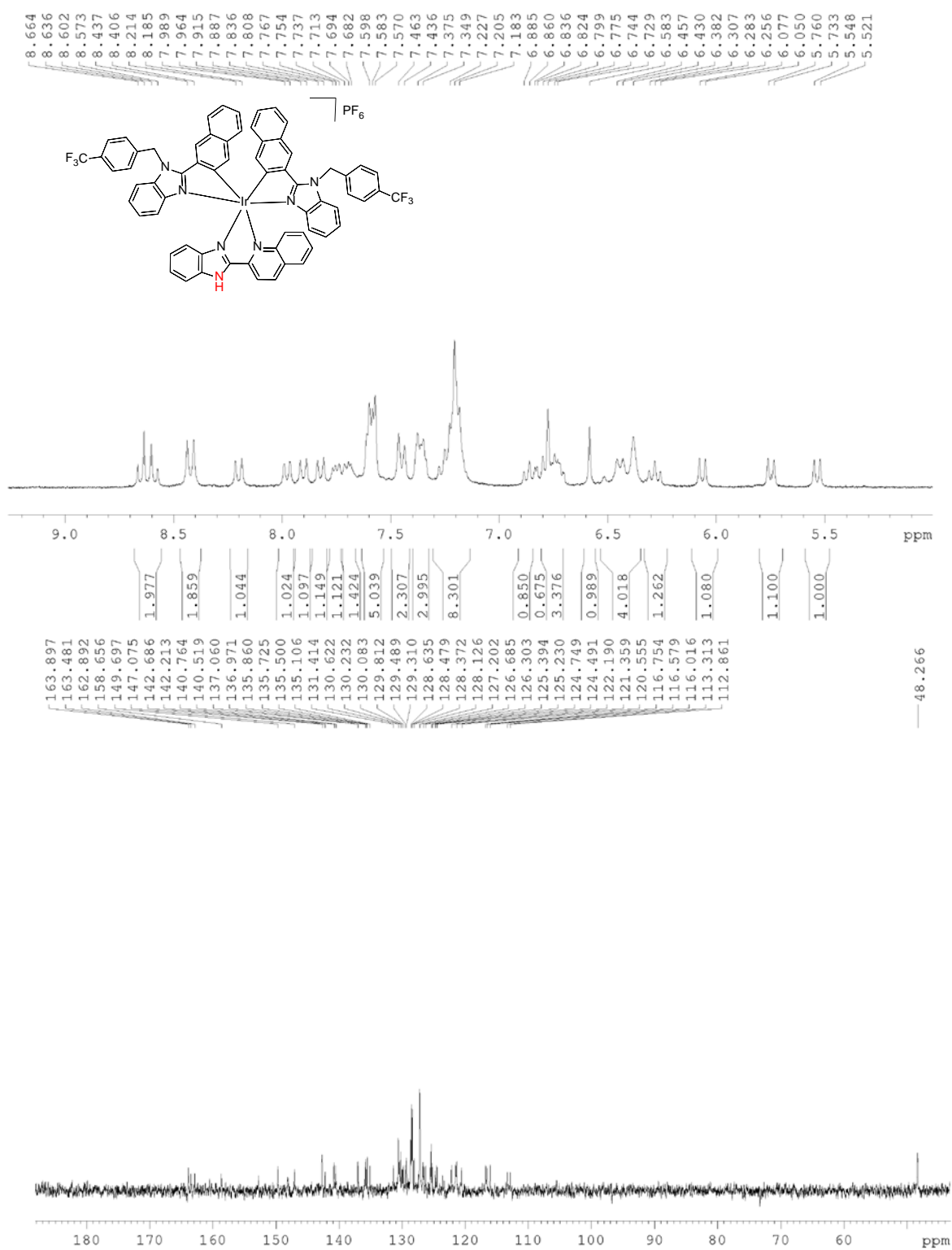


Figure S3. ¹H and ¹³C NMR in [D₆]DMSO for **3**.

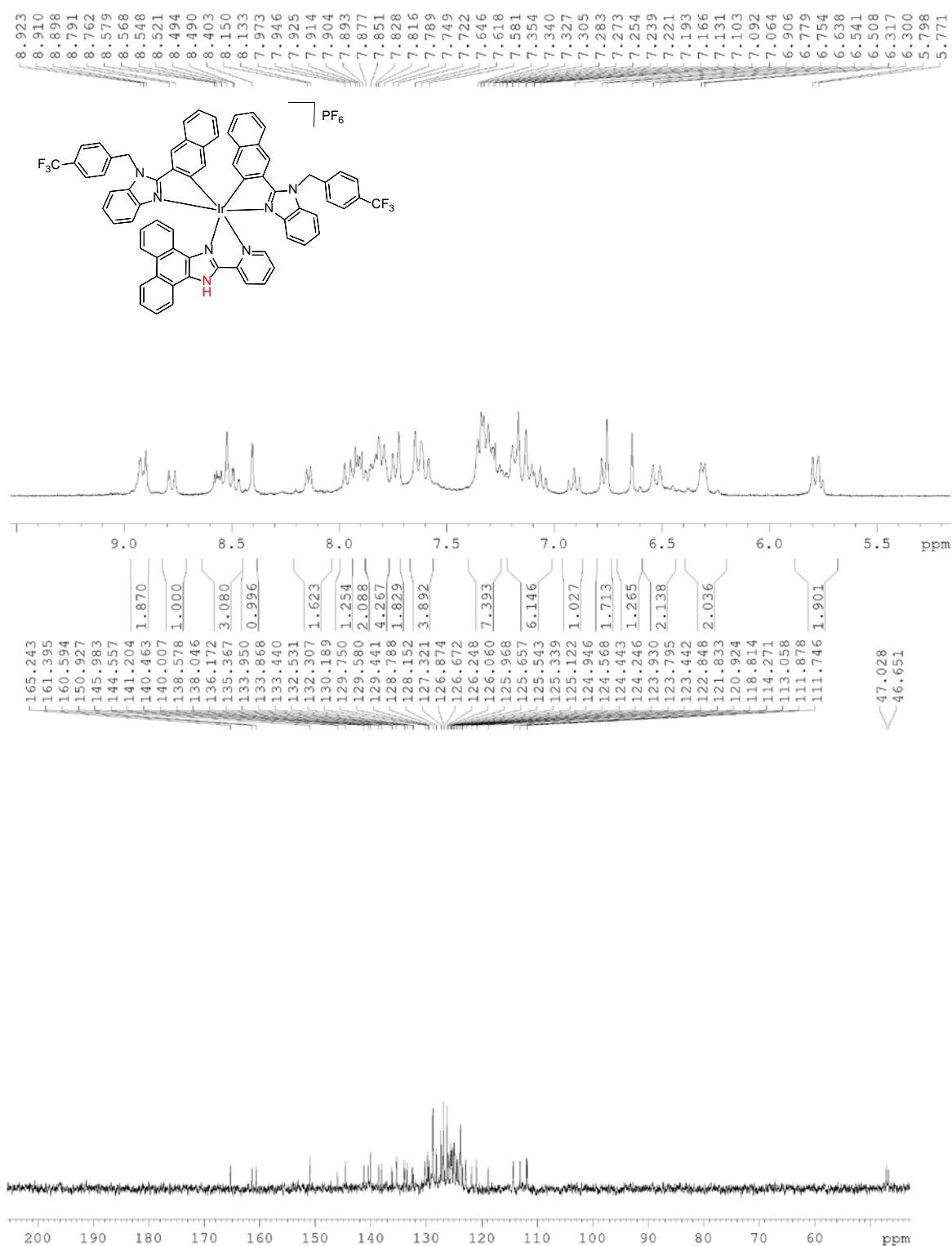


Figure S4. ¹H and ¹³C NMR in [D₆]DMSO for **4** at 70°C.

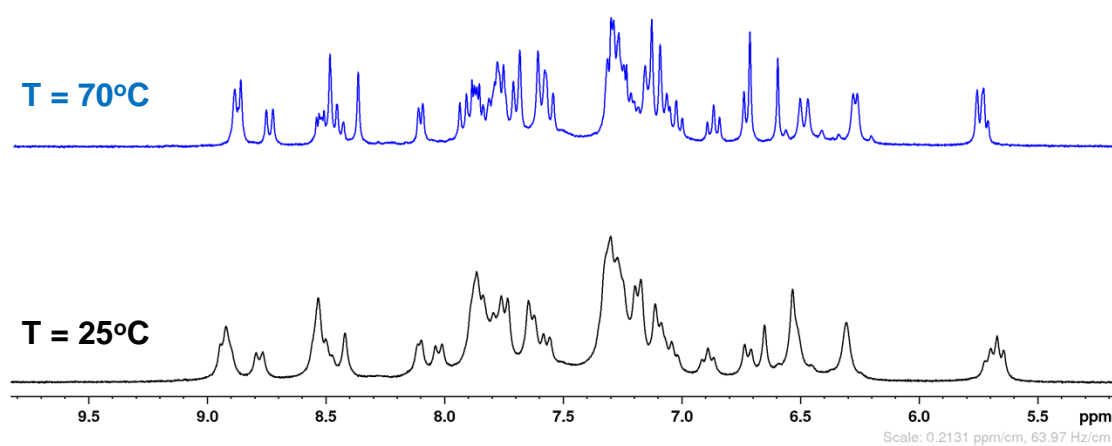


Figure S5. ¹H NMR in [D₆]DMSO for **4** at 70°C (top) and 25°C (bottom).

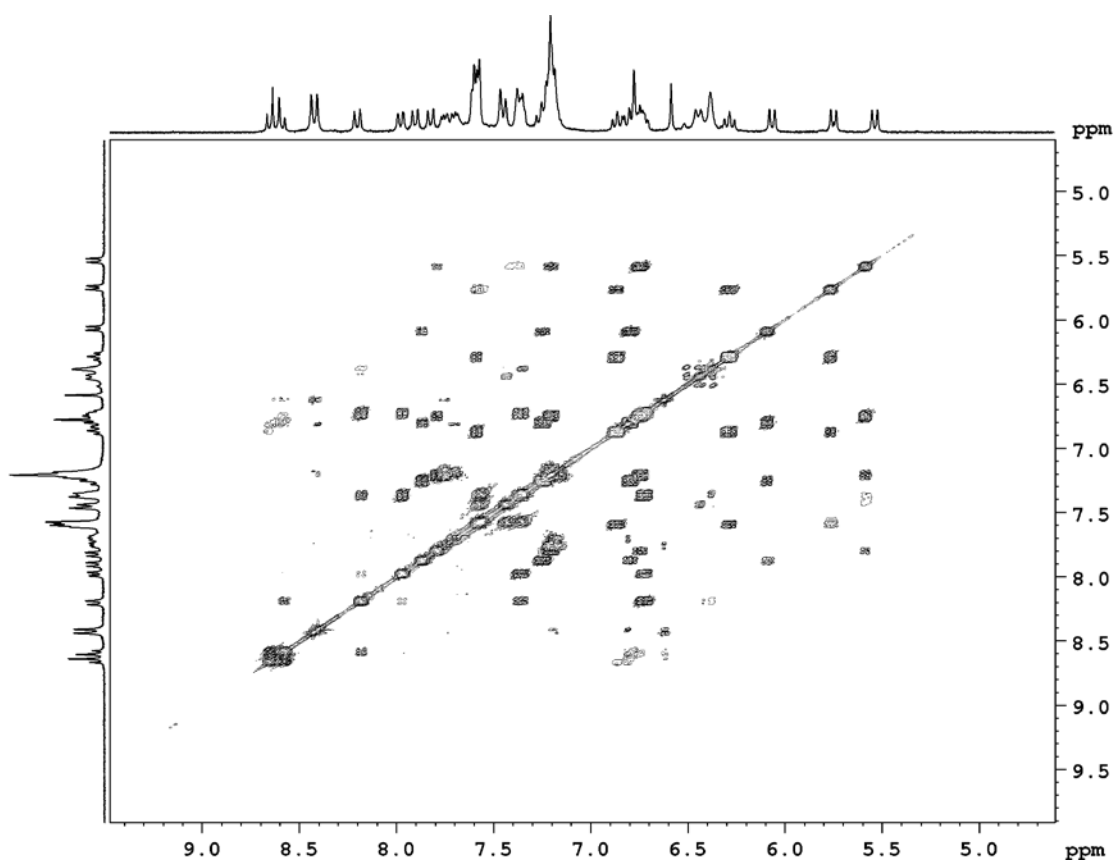


Figure S6. COSY 2D ^1H - ^1H NMR of complex **3**.

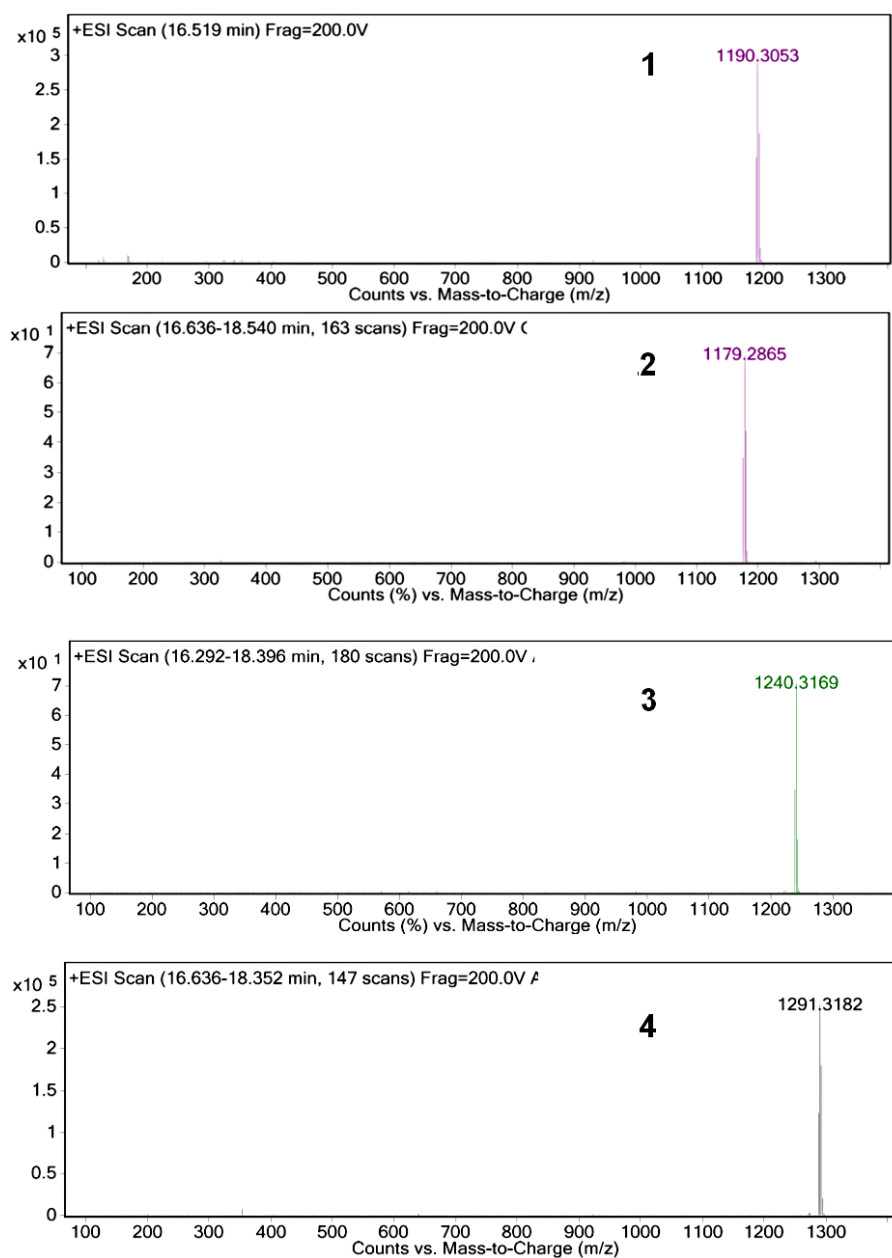


Figure S7. Positive-ion ESI-MS of complexes **1-4**.

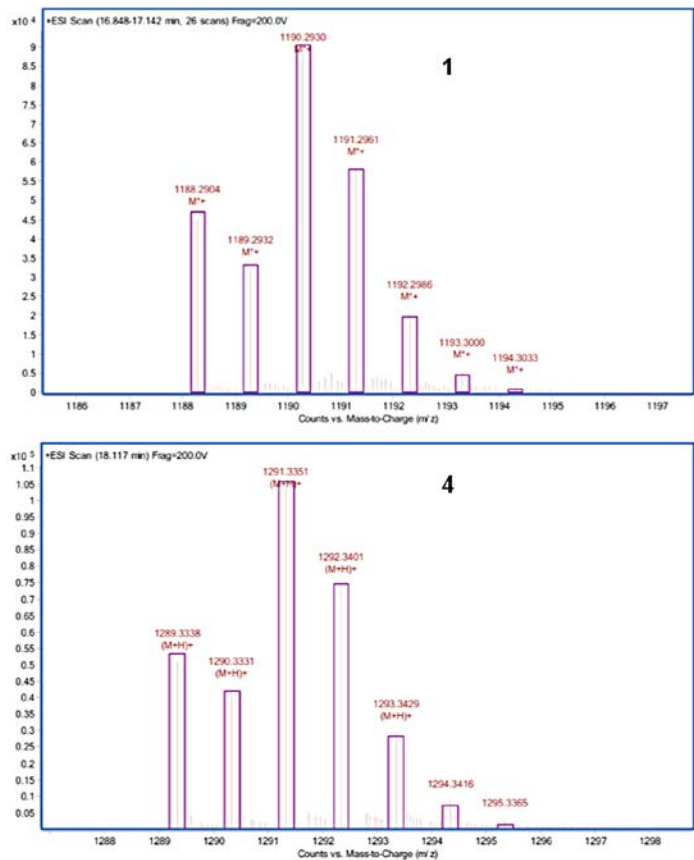


Figure S8. Theoretic vs experimental molecular ion $[M-PF_6]^+$ of **1** and **4**.

Table S1. HPLC method

Time (min)	0.1% formic acid in dH ₂ O	0.1% formic acid in CH ₃ CN
0-14	90	10
14-19.5	10	90
19.6-24	90	10

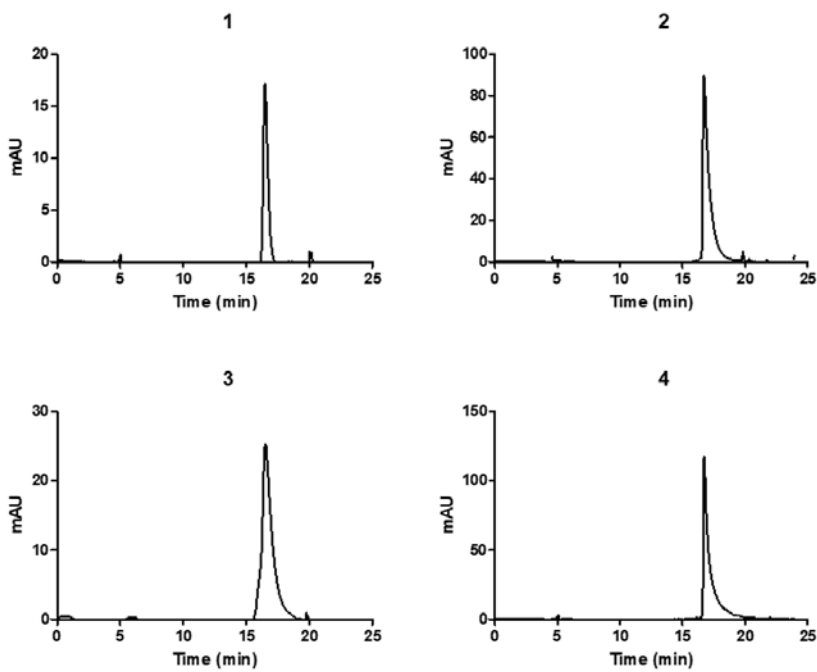


Figure S9. HPLC chromatograms of **1-4** in DMSO.

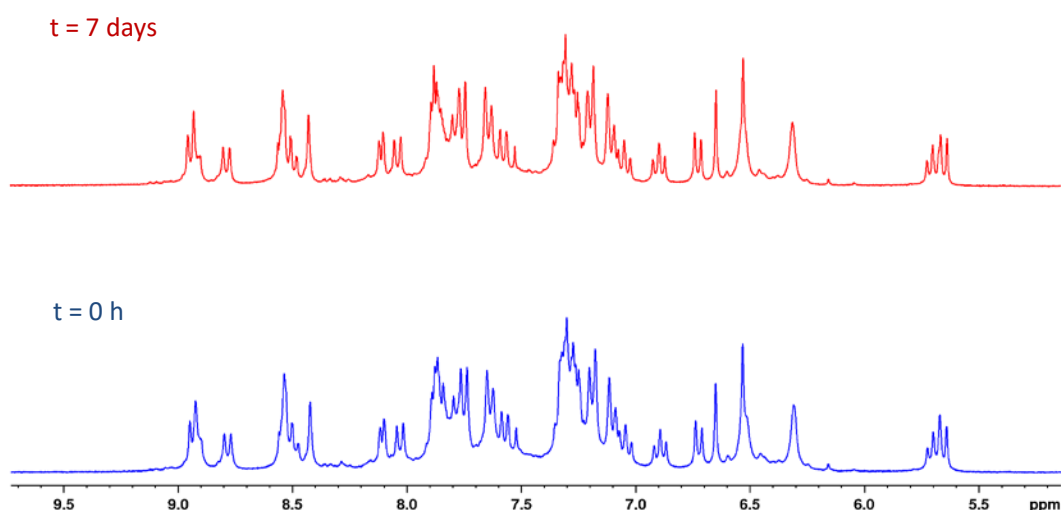


Figure S10. ^1H NMR spectra of **3** measured after dissolving immediately in $\text{DMSO}[D_6]$ (bottom) and after 7 days (up) at RT.

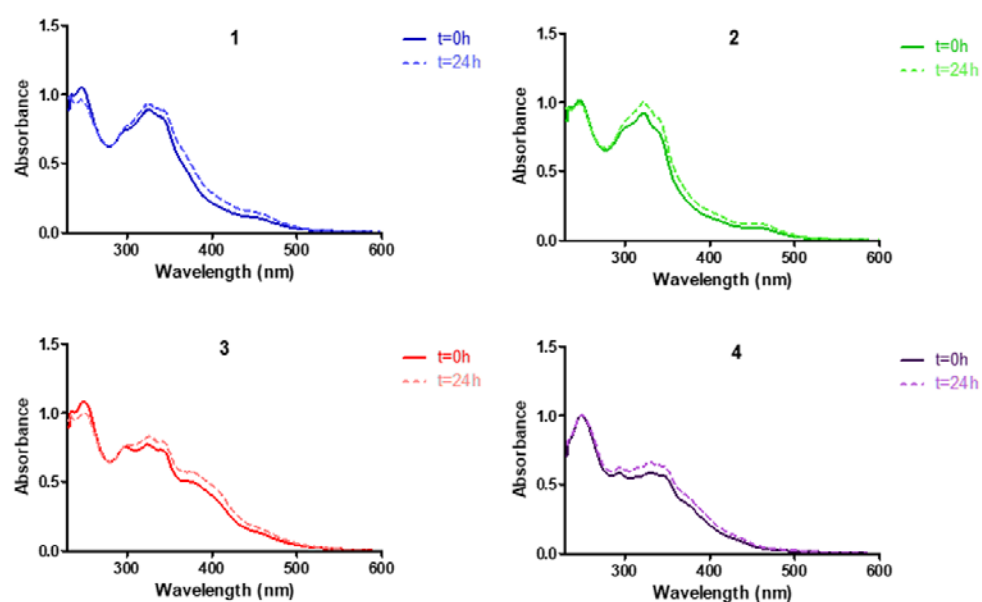


Figure S11. UV-Vis spectra of complexes **1-4** showing the stability in RPMI cell culture medium (1% DMSO).

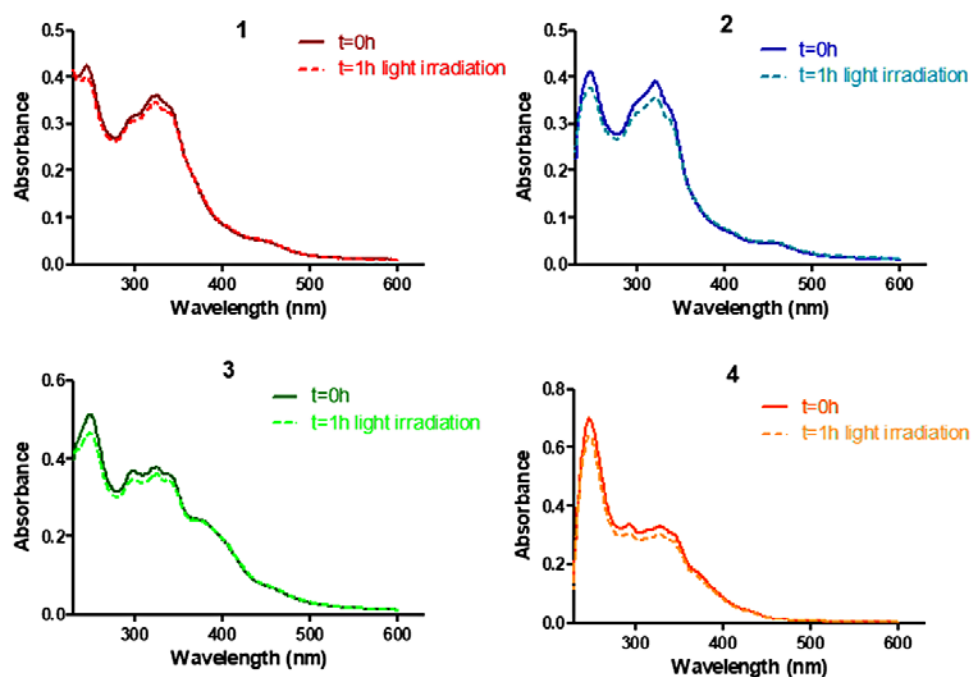


Figure S12. Photostability: UV-Vis spectra of complexes **1-4** before and after light exposure.

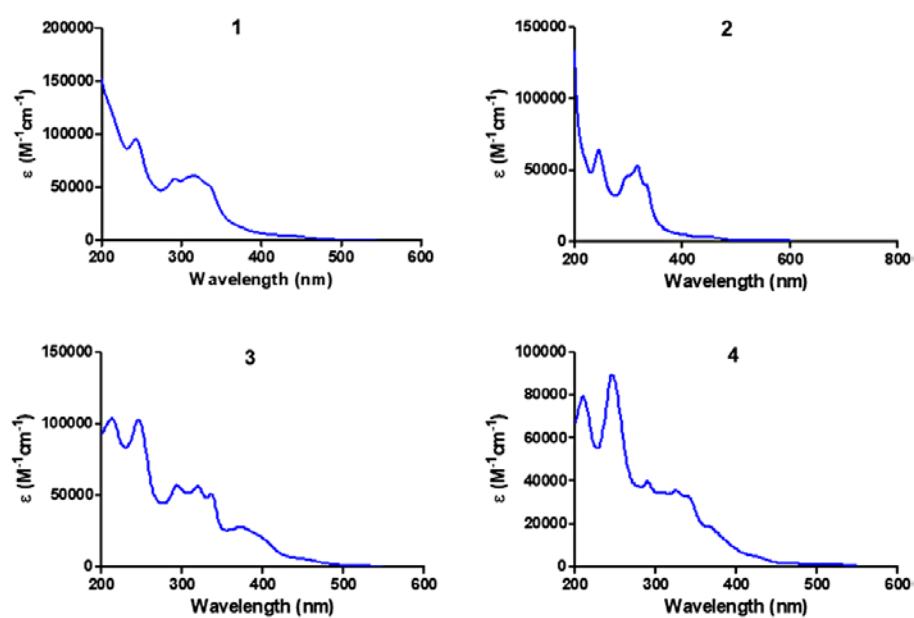


Figure S13. UV/Vis absorption spectra of **1-4** in acetonitrile.

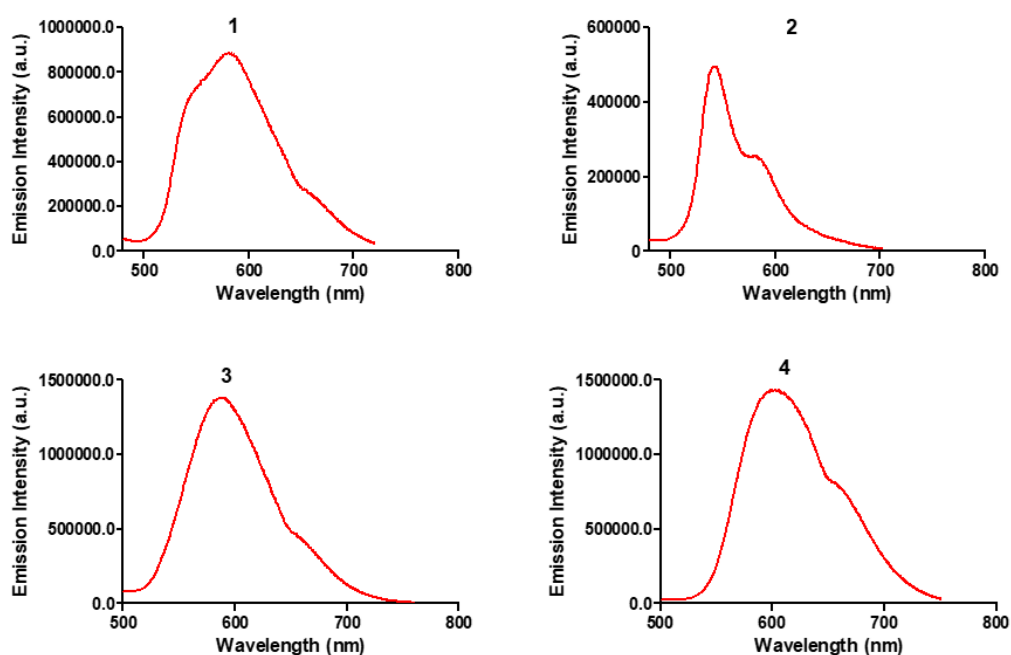


Figure S14. Emission spectra of complexes in aerated acetonitrile. λ_{exc} = 370, 360, 390 and 403 nm respectively.

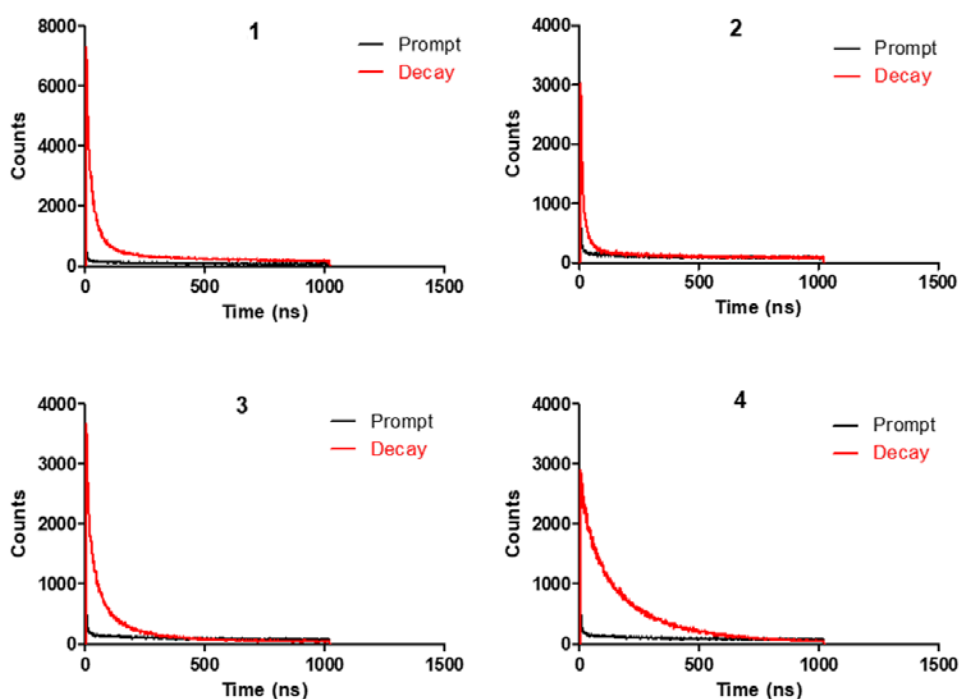


Figure S15. Emission decay kinetics of complexes in water (1% DMSO).

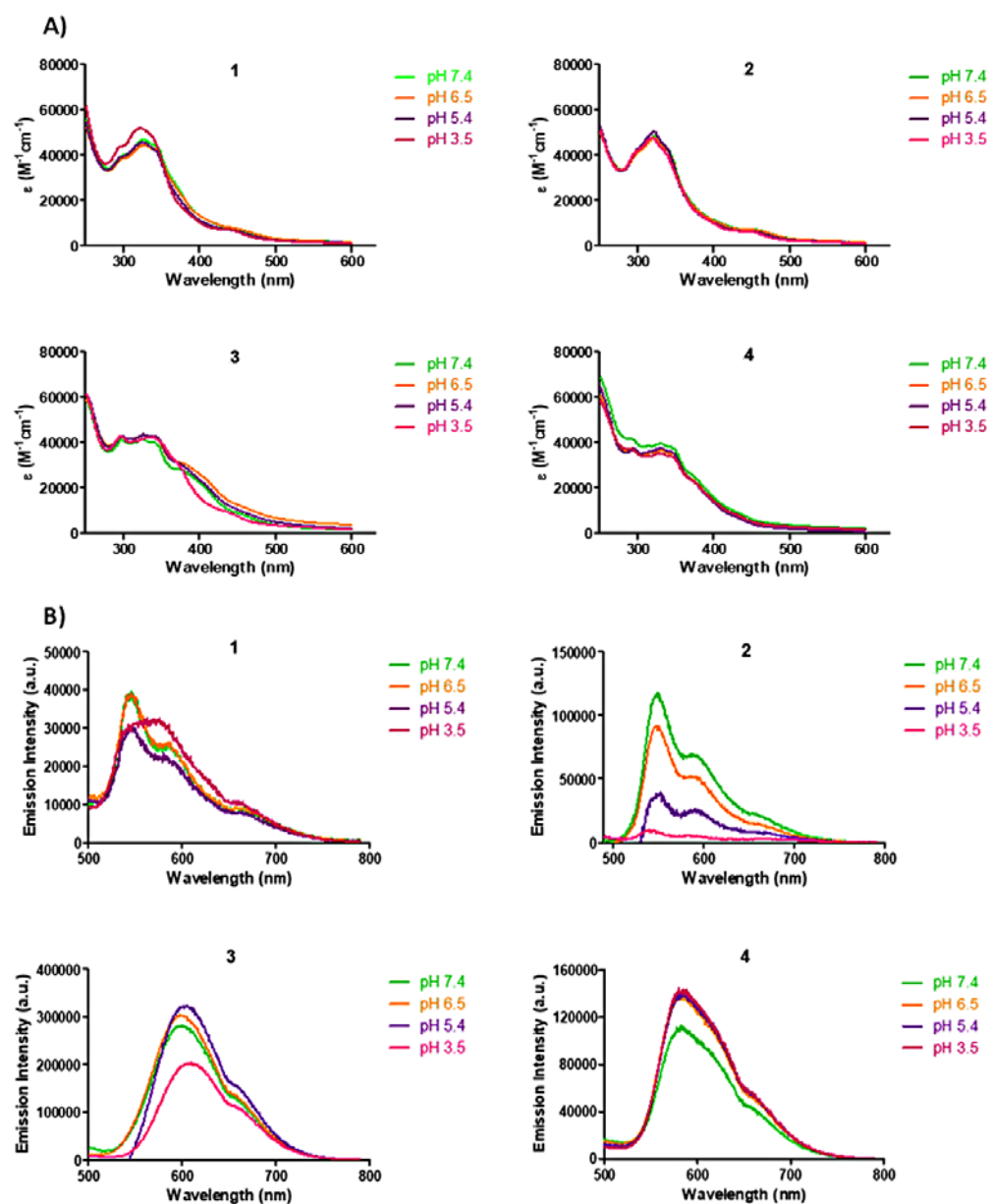


Figure S16. A) UV/Vis absorption spectra and B) emission spectra of **1-4** in buffer/DMSO (99:1) at different pH. The excitation wavelength was 405 nm.

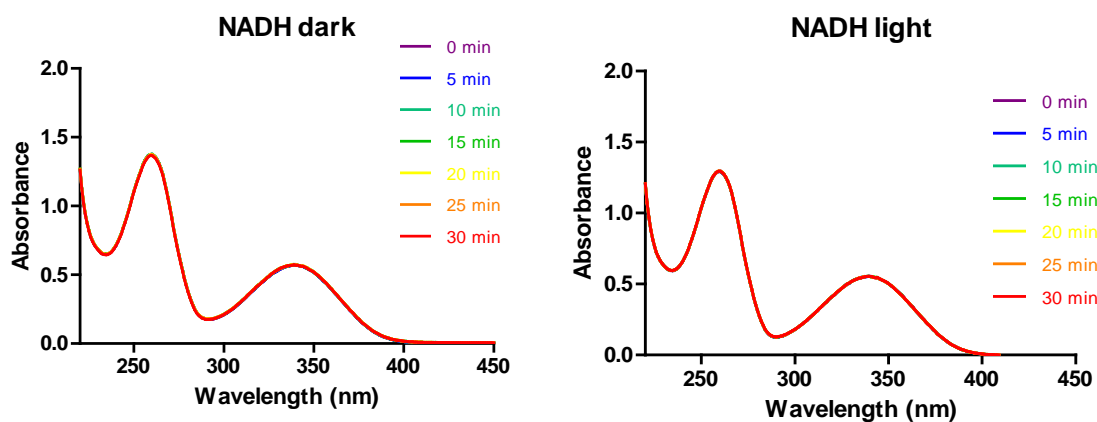


Figure S17. Stability of NADH in the dark and under light irradiation (465 nm, 8.4 mW/cm²) after 30 min.

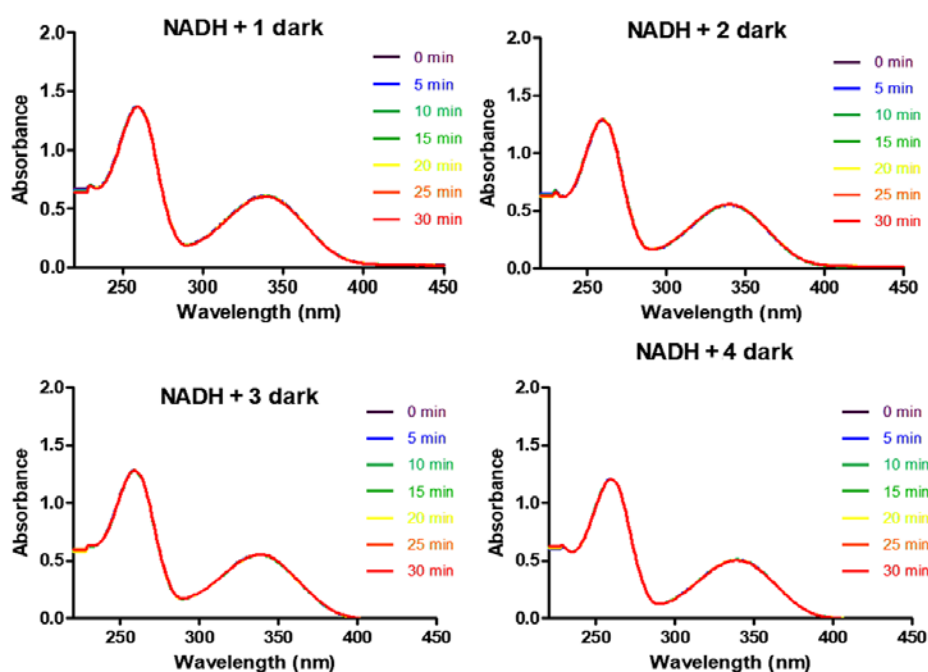


Figure S18. UV/Vis spectra of NADH (100 μ M) in presence of complexes (5 μ M) in the dark for 30 min.

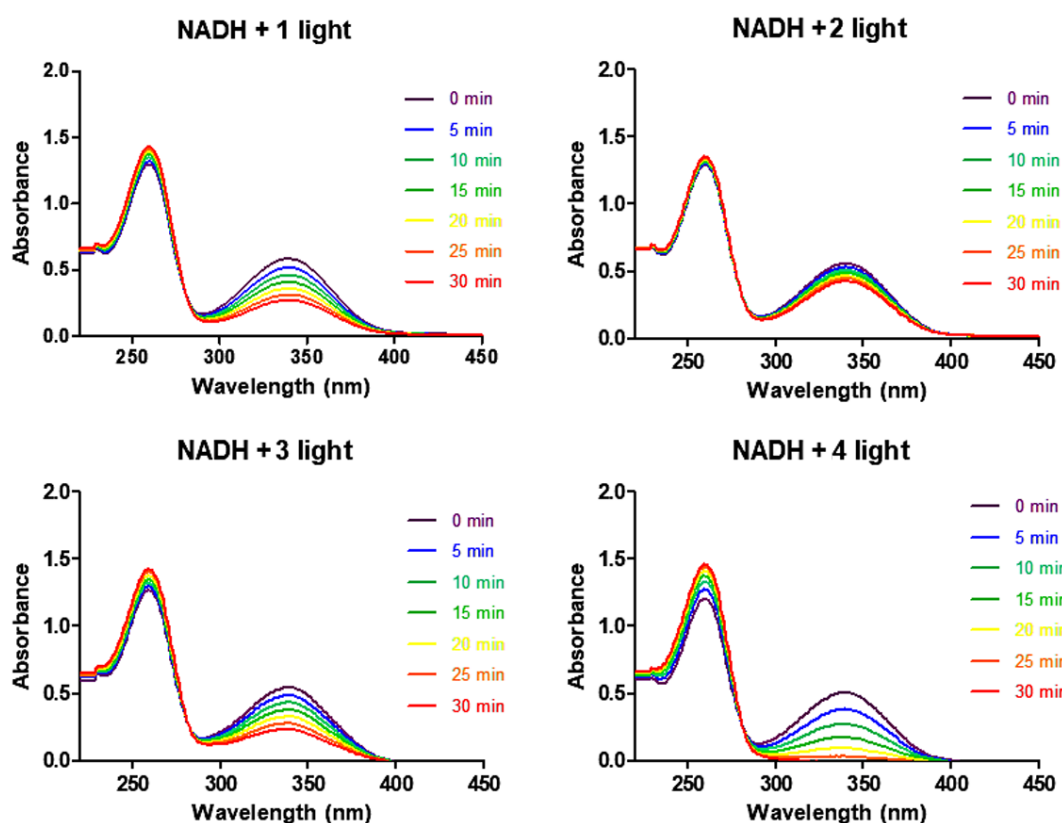


Figure S19. UV/Vis spectra of NADH (100 μ M) in presence of complexes (5 μ M) under 465 nm blue light irradiation for 30 min.

Table S2. TON and TOF of compounds **1-4**. TON was defined as the number of moles of NADH that Ir compound could convert in 30 min. TOF was calculated from the concentration of oxidized NADH (calculated by the difference of concentration of NADH) after 30 min divided by the concentration of complexes.

Compound	TON	TOF ($\times 10^4$) (s^{-1})	TOF (h^{-1})
1	10.1	55.9	20.1
2	4.2	23.2	8.3
3	9.9	55.5	20.0
4	16.4	91.3	32.9

Table S3. Log P values of **2a** measured using the “shake flask” method and the HPLC-method designed by Keppler *et al.*⁷ at room temperature.

Method	φ_0	$\log P^a$
Shake flask (ICP-MS)	-	2.6 ± 0.1
HPLC-based method	76.7	2.3 ± 0.1

^aResults are expressed as the mean \pm SD from two independent experiments.

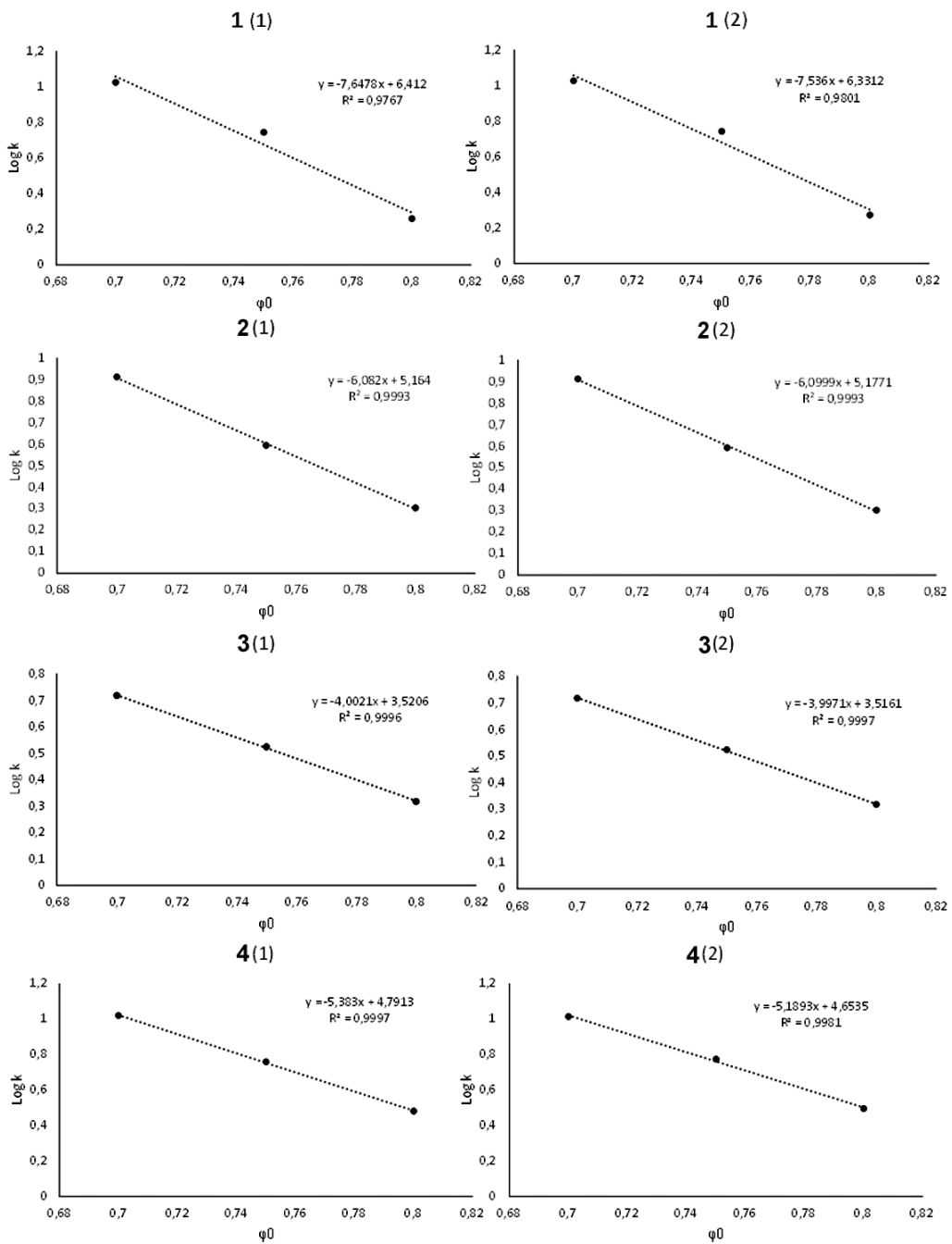


Figure S20. Soczewinski-Snyder relationship for **1-4** of two independent experiments.

Table S4. Mean chromatographic hydrophobicity parameter φ_0 calculated using Soczewinski-Snyder relationship when Log k = 0.

Compound	φ_0
1	84
2	84
3	88
4	89

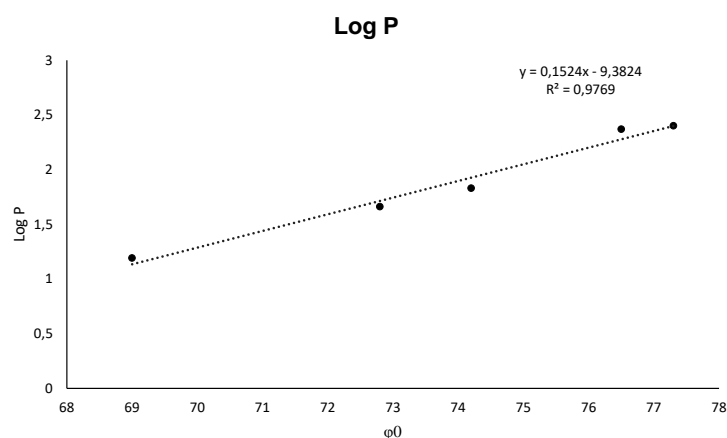


Figure S21. Graphic representation of the log P of the most lipophilic complexes found by Keppler *et al.* and their corresponding values of ϕ_0 .

Table S5. IC₅₀ values^a (μM) obtained for HeLa cervical cancer cells treated with the investigated Ir complexes in the dark or after irradiation by visible light (1 h, $\lambda_{\text{max}} = 420 \text{ nm}$, $77 \pm 3 \text{ Wm}^{-2}$) determined by the MTT assay in normoxic or hypoxic conditions.

HeLa	Normoxia			Hypoxia		
	dark	420 nm	PI ^b	dark	420 nm	PI ^b
1	>300	13 ± 2	>22	>300	17±3	>17
2	>300	>50		>300	>50	
3	>300	9.7 ± 0.9	>31	>300	18±5	>17
4	>300	4.5 ± 0.6	>66	>300	6±2	>49

^aData represent the mean ± SD from three independent experiments, each made in triplicate. ^bPI (phototoxic index) = [IC₅₀]_{dark}/[IC₅₀]_{420 nm}.

Table S6. IC₅₀ values (μM) obtained for A375, 518.A2 melanoma and HeLa cervical cancer cells treated with the investigated Ir complexes in the dark or after irradiation by visible light (1 h, $\lambda_{\text{max}} = 420 \text{ nm}$, $77 \pm 3 \text{ Wm}^{-2}$) determined by Neutral Red assay in normoxic condition.

	A375		518.A2		HeLa	
	dark	420 nm	dark	420 nm	dark	420 nm
1	>50	16 ± 2	>50	11.4 ± 0.5	>50	20 ± 3
2	>50	>50	>50	48 ± 2	>50	>50
3	>50	13.8 ± 0.8	>50	8 ± 1	>50	17 ± 4
4	>50	5.9 ± 0.1	>50	3.3 ± 0.2	>50	6.5 ± 0.9

^aData represent the mean ± SD from two independent experiments, each made in triplicate.

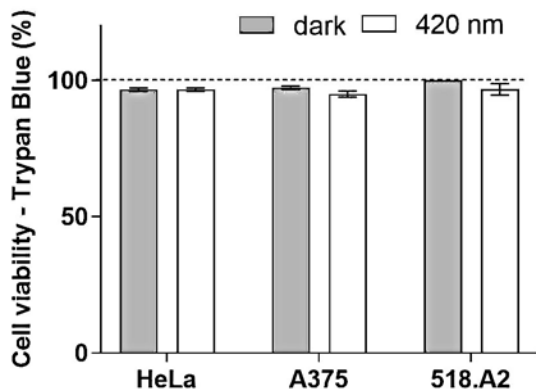


Figure S22. Viability of untreated cells non-irradiated (dark) or after irradiation by blue light for 1 h (420 nm) after 72 h recovery measured with the aid of trypan blue assay. Results are presented as mean ± SD from three independent experiments. Non-irradiated control cells were taken as 100%.

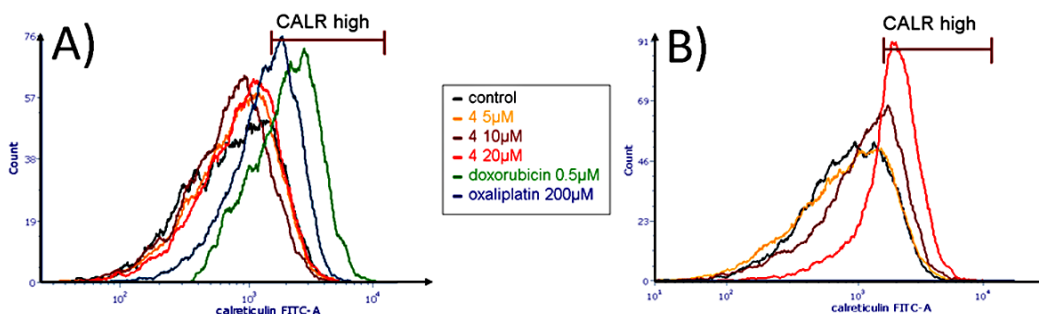


Figure S23. Representative flow cytometry histograms of ecto-Calreticulin exposure for A375 cells treated with the tested complexes (**4**, doxorubicin, oxaliplatin) in the dark (A) and after irradiation (B).

Table S7. Ecto-CALR exposing population (%) obtained from flow cytometry histograms.

	DARK	IRRADIATED
control	16.8	16.6
4 (5 μ M)	14.7	17.2
4 (10 μ M)	9.9	27.9
4 (20 μ M)	16.6	60.1
doxorubicin (0.5 μ M)	63.7	ND
oxaliplatin (200 μ M)	41.2	ND

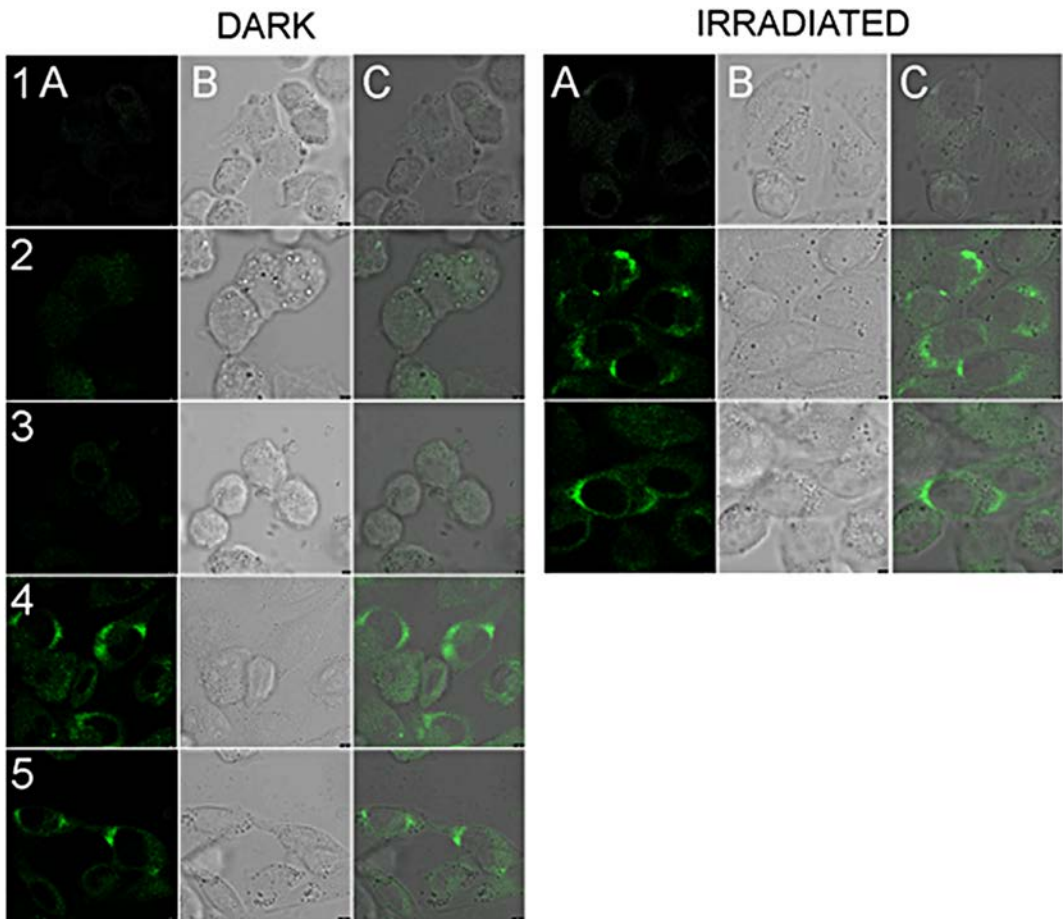


Figure S24. Immunofluorescence analysis of calreticulin exposure by confocal microscopy. A375 cells were untreated (panels 1) or treated with **4** (10 μ M panels 2, 20 μ M panels 3), doxorubicin (0.5 μ M – panels 4) or oxaliplatin (200 μ M – panels 5) followed by irradiation with blue light (420nm, 1 h) or kept in the dark with subsequent incubation for 22 h in the drug-free medium in the dark. Channels: A. Fluorescence signal from CRT-Alexa fluor 488 conjugate. B. Bright field. C. Merge of the fluorescence and bright field channels.

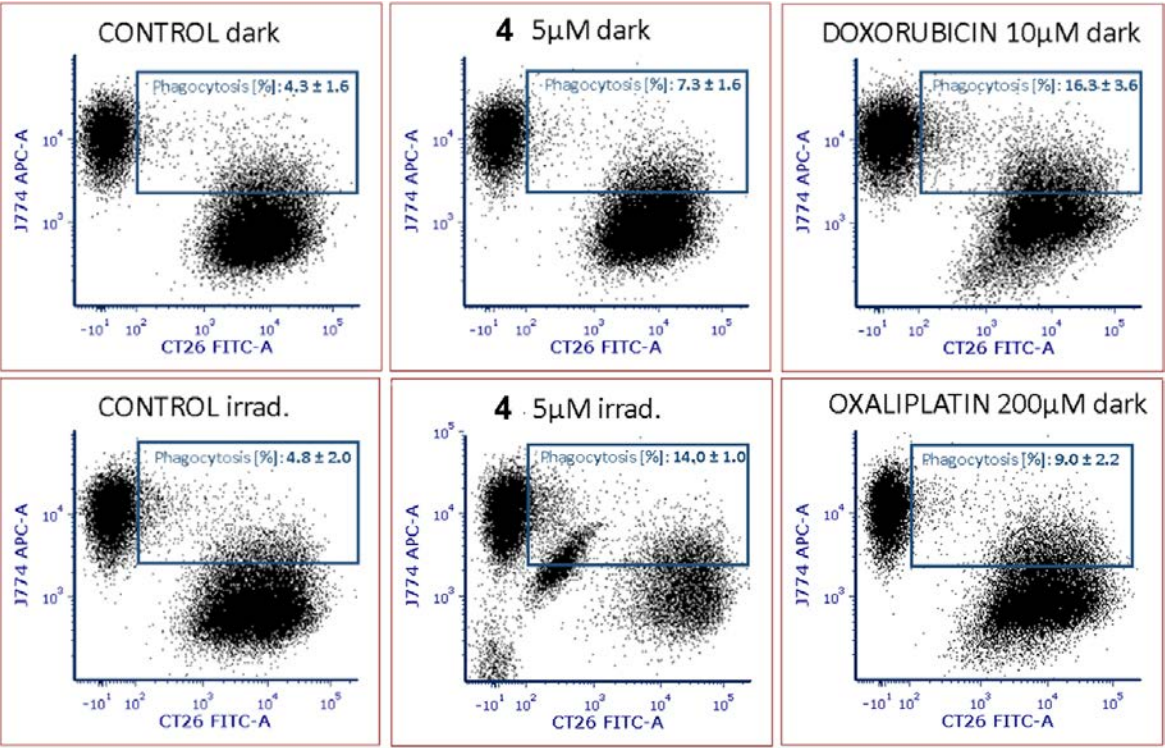


Figure S25. Phagocytosis assay CT26/J774.A1. Murine cancer cells CT26 (non-treated or pretreated with **4**, doxorubicin, or oxaliplatin) were stained with CellTracker™ green CMFDA and co-incubated with pre-stained (CellTracker™ red CMTX) murine macrophages J774.A1. The cell mixture was analyzed by flow cytometry. Double-stained macrophages indicate phagocytosis.

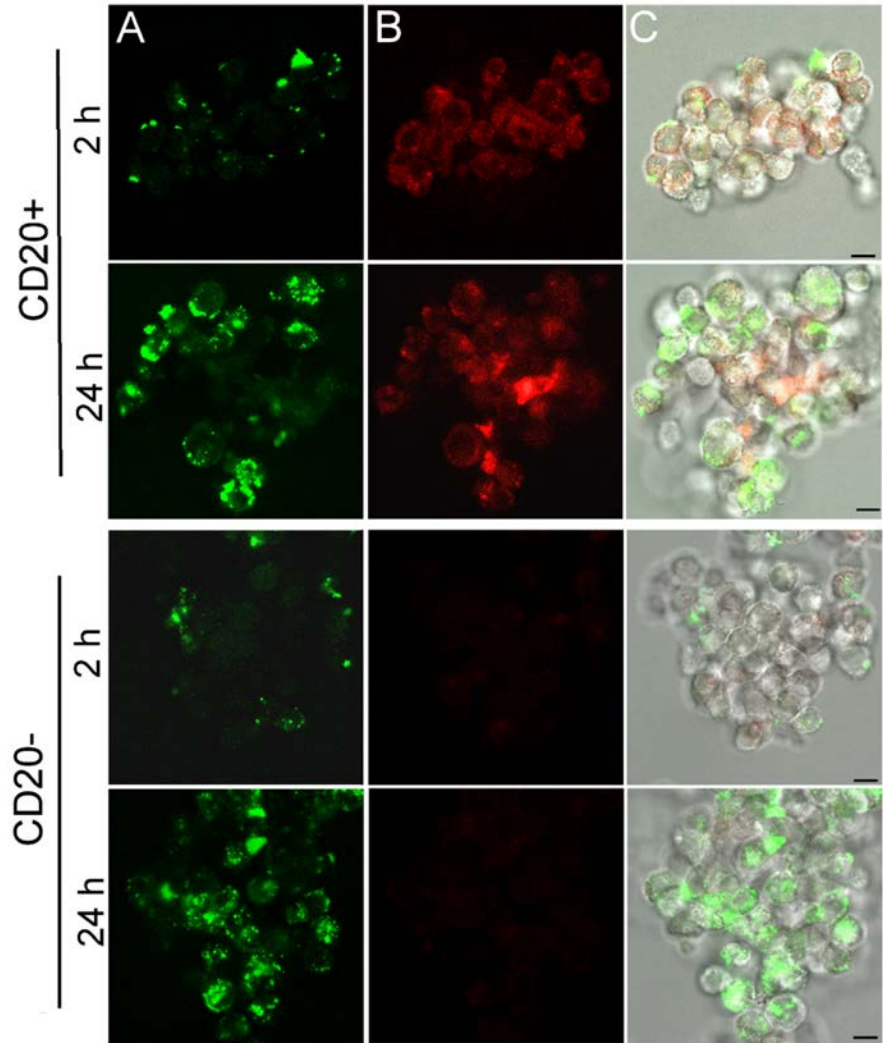


Figure S26. Penetration of complex **4** into 3D spheroids generated from A375CD20+ and A375CD20- cells. Cell spheroids (diameter: 40 – 60 μ m) were treated with complex **4** (10 μ M) and incubated for 2 h or 24 h in the dark. Spheroids were subsequently fixed and stained with APC anti-human CD20 antibody. Channels: Panels A, phosphorescence from complex **4**. Panels B, CD20 antibody. Panels C, overlay of the fluorescence channels and bright field. Scale bar represents 10 μ m.

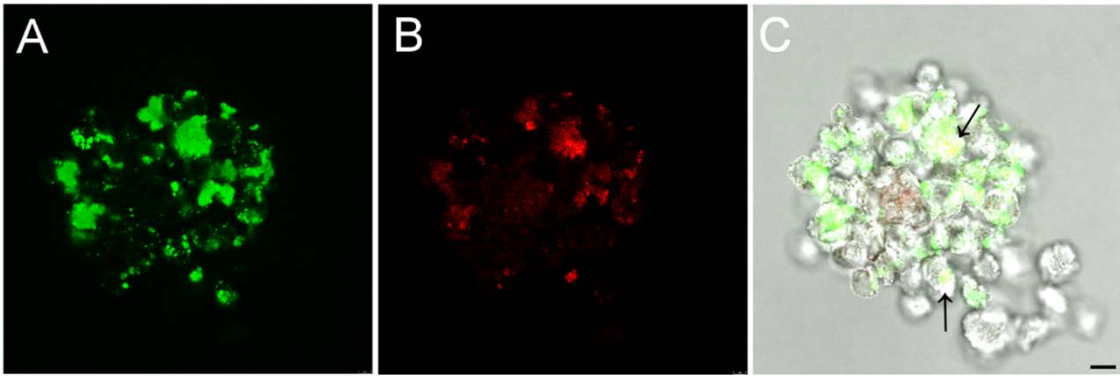


Figure S27. Penetration of complex **4** to 3D spheroid generated from unsorted A375 cells. Spheroids (diameter: 80 μm) were treated with complex **4** (10 μM) and incubated in the dark for 24 h. After washing, cells were co-stained with APC anti-human CD20 antibody (Miltenyi Biotec). Channels: Panel A, phosphorescence from complex **4**. Panel B, CD20 antibody. Panel C, overlay of the fluorescence channels and bright field. Arrows indicate the co-stained areas. Scale bar represents 10 μm .

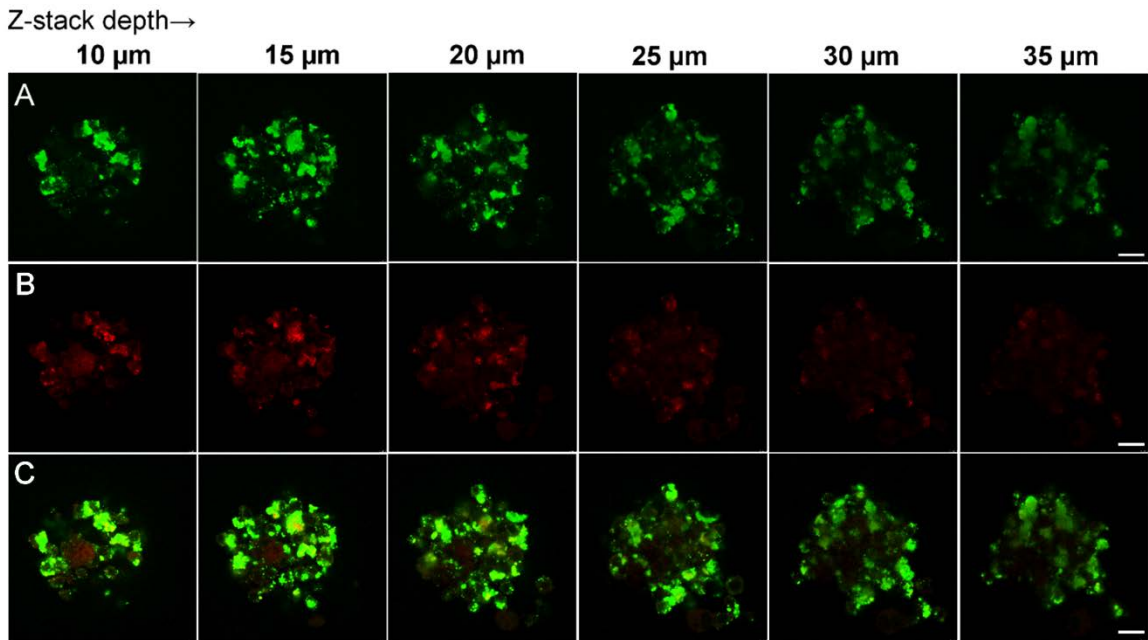


Figure S28. Penetration of complex **4** to 3D spheroid generated from unsorted A375 cells. Spheroids (diameter: 80 μm) were treated with complex **4** (10 μM) and incubated in the dark for 24 h. After washing, cells were co-stained with APC anti-human CD20 antibody (Miltenyi Biotec). Channels: Panels A, phosphorescence from complex **4**. Panels B, CD20 antibody. Panels C, overlay of the fluorescence channels. Confocal z-stacks were acquired in defined steps (10-35 μm). Scale bar represents 20 μm .

SMILES

1;FC(C(C=C1)=CC=C1CN2C3=C(C=CC=C3)[N]([Ir]456([N]7=C(C8=C6C=C(C=CC=C9)C9=C8)N(C%10=C7C=CC=C%10)CC(C=C%11)=CC=C%11C(F)(F)F)[N]%12=CC=CC=C%12C%13=[N]5C(C=CC=C%14)=C%14N%13)=C2C%15=C4C=C%16C(C=CC=C%16)=C%15)(F)F.FP(F)(F)(F)(F)F

2;FC(C(C=C1)=CC=C1CN2C3=C(C=CC=C3)[N]([Ir]456([N]7=C(C8=C6C=C(C=CC=C9)C9=C8)N(C%10=C7C=CC=C%10)CC(C=C%11)=CC=C%11C(F)(F)F)[N](C(C=CC=C%12)=C%12N%13)=C%13C%14=[N]5C=CN%14)=C2C%15=C4C=C%16C(C=CC=C%16)=C%15)(F)F.FP(F)(F)(F)(F)F

3;FC(C(C=C1)=CC=C1CN2C3=C(C=CC=C3)[N]([Ir]456([N]7=C(C8=C6C=C(C=CC=C9)C9=C8)N(C%10=C7C=CC=C%10)CC(C=C%11)=CC=C%11C(F)(F)F)[N]%12=C%13C(C=CC=C%13)=CC=C%12C%14=[N]5C(C=CC=C%15)=C%15N%14)=C2C%16=C4C=C%17C(C=CC=C%17)=C%16)(F)F.FP(F)(F)(F)(F)F

4;FC(C(C=C1)=CC=C1CN2C3=C(C=CC=C3)[N]([Ir]456([N]7=C(C8=C6C=C(C=CC=C9)C9=C8)N(C%10=C7C=CC=C%10)CC(C=C%11)=CC=C%11C(F)(F)F)[N]%12=CC=CC=C%12C%13=[N]5C(C(C=CC=C%14)=C%14C%15=C%16C=CC=C%15)=C%16N%13)=C2C%17=C4C=C%18C(C=CC=C%18)=C%17)(F)F.FP(F)(F)(F)(F)F